Sheared flows and transition to improved confinement regime in the TJ-II stellarator

2009 Plasma Phys. Control. Fusion 51 124015

(http://iopscience.iop.org/0741-3335/51/12/124015)

Plasma Phys. Control. Fusion **51** (2009) 124015 (11pp) doi:10.1088/0741-3335/51/12/124015

Sheared flows and transition to improved confinement regime in the TJ-II stellarator

T Estrada[1], T Happel[1], L Eliseev[2], D López-Bruna[1], E Ascasíbar[1], E Blanco[1], L Cupido[3], J M Fontdecaba[1], C Hidalgo[1], R Jiménez-Gómez[1], L Krupnik[4], M Liniers[1], M E Manso[3], K J McCarthy[1], F Medina[1], A Melnikov[2], B van Milligen[1], M A Ochando[1], I Pastor[1], M A Pedrosa[1], F L Tabarés[1], D Tafalla[1] and TJ-II Team[1]

[1] Laboratorio Nacional de Fusión. As. EURATOM-CIEMAT, 28040 Madrid, Spain
[2] Institute of Nuclear Fusion, RNC Kurchatov Institute, Moscow, Russia
[3] Instituto de Plasmas e Fusao Nuclear. As. EURATOM-IST, Lisboa, Portugal
[4] Institute of Plasma Physics, NSC KIPT, 310108 Kharkov, Ukraine

Received 18 June 2009, in final form 30 July 2009
Published 10 November 2009
Online at stacks.iop.org/PPCF/51/124015

Abstract
Sheared flows have been experimentally studied in TJ-II plasmas. In low-density ECH plasmas, sheared flows can be easily controlled by changing the plasma density, thereby allowing the radial origin and evolution of the edge velocity shear layer to be studied. In high density NBI heated plasmas a negative radial electric field is observed that is dominated by the diamagnetic component. The shear of the negative radial electric field increases at the L–H transition by an amount that depends on the magnetic configuration and heating power. Magnetic configurations with and without a low order rational surface close to the plasma edge show differences that may be interpreted in terms of local changes in the radial electric field induced by the rational surface that could facilitate the L–H transition. Fluctuation measurements show a reduction in the turbulence level that is strongest at the position of maximum E_r shear. High temporal and spatial resolution measurements indicate that turbulence reduction precedes the increase in the mean sheared flow, but is simultaneous with the increase in the low frequency oscillating sheared flow. These observations may be interpreted in terms of turbulence suppression by oscillating flows, the so-called zonal flows.

(Some figures in this article are in colour only in the electronic version)

1. Introduction

During the last two decades, theoretical and experimental investigations have accumulated substantial evidence to show that turbulence de-correlation by sheared flows is the mechanism

that leads to a strong reduction in turbulence and the formation of transport barriers. This mechanism was proposed in 1990 [1] and confirmed experimentally in the DIII-D tokamak [2]. At present most experimental evidence strongly supports the paradigm of sheared electric field suppression of turbulence to explain the H-mode reduced transport, although the underlying mechanism that generates the electric fields is one of the fundamental open issues confronting the fusion community. More recently, the relevance of zonal flows on turbulence regulation and formation of transport barriers has been identified [3, 4].

The H-mode develops in both tokamaks and stellarators across a wide plasma parameter range [5]. Helical devices provide valuable contributions to H-mode physics due to their distinctive characteristics, i.e. low/high magnetic shear, magnetic field ripple and neoclassical ambipolar electric field [6].

In the TJ-II stellarator, sheared flows can be easily driven and damped at the plasma edge by changing the plasma density. Besides, spontaneous L–H mode transitions have been achieved [7], when operating under lithium coated walls [8] and with NBI heating. TJ-II is, therefore, a suitable plasma physics laboratory to contribute to the understanding of the physics of shear flow development in fusion plasmas.

2. Experimental set-up

TJ-II is a helical device with major radius $R = 1.5$ m, minor radius $\langle a \rangle \leqslant 0.22$ m and magnetic field $B_0 < 1.2$ T. TJ-II offers the possibility to explore a wide rotational transform range in low, negative magnetic shear configurations. Plasmas are started up and heated by ECH 2nd harmonic using two gyrotrons at 53.2 GHz with X-mode polarization. The maximum power per gyrotron is 300 kW and the power density is about 10 W cm^{-3} [9]. Under these heating conditions the plasma density has to be kept below the cut-off value of 1.75×10^{19} m^{-3}. Higher density plasmas are achieved using NBI heating. Two injectors, one *co*- and one *counter*-, are in operation delivering a port-through power per injector up to 500 kW. The experimental results presented below were obtained in hydrogen plasmas.

A two-channel Doppler reflectometer [10], recently installed in TJ-II, is used to experimentally investigate radial electric fields and turbulence dynamics. As has been shown in the W7-AS stellarator, this diagnostic technique allows the measurement of the perpendicular rotation velocity and density fluctuations with good spatial and temporal resolution [11]. Besides, measurements made simultaneously at two different radial positions, such as those carried out in the ASDEX Upgrade tokamak [12], allow information on the temporal evolution of the radial electric field and its shear to be obtained. Additionally, a heavy ion beam probe (HIBP) diagnostic [13] and two sets of multi-Langmuir probes [14] are also used. The Langmuir probes are toroidally separated by 160° and the field line passing through one of the probes is 150° poloidally apart when reaching the toroidal position of the second probe that is more than 5 m away. This arrangement allows the measurement of different edge plasma parameters and their long distance correlation properties.

3. Development of the negative radial electric field

In low-density ECH plasmas ($\langle n_e \rangle \leqslant 1.2 \times 10^{19}$ m^{-3}), the formation of a negative radial electric field at the plasma edge was first detected using Langmuir probes [15] and later confirmed using microwave reflectometry [16] and a HIBP [17]. It has been shown that the radial electric field reverses spontaneously as the line-averaged density reaches a certain threshold density that depends on heating power and magnetic configuration. Experimentally, the plasma density is

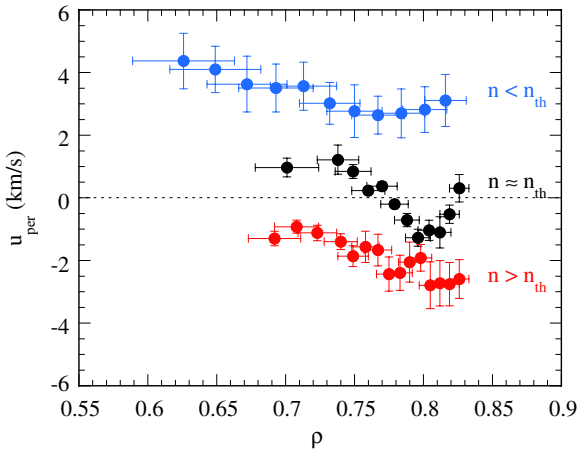

Figure 1. Radial profiles of the perpendicular rotation velocity measured by Doppler reflectometry in ECH plasmas at densities below, close to and above the threshold density. The line-averaged plasma densities are 0.5, 0.7 and 0.9 $\times$ 10^{19} m^{-3}, respectively, and the ECH power is 500 kW.

tuned along the discharge by using a pre-programmed gas puffing system. Measurements with the two-channel reflectometer show that the radial origin of the edge shear layer is linked to the plasma region with maximum density gradient expanding radially and being detected by the Langmuir probes at the plasma edge, as the density increases above the threshold value [18]. These results suggest a two-step process in edge shear formation: first, a seeding mechanism linked to plasma gradients and, second, an amplification process linked to plasma turbulence. Langmuir probes detect long-range correlations in the plasma potential that are amplified as the velocity shear expands to the plasma edge, whereas density fluctuations are always dominated by short-range scales [14]. The radial profiles of the perpendicular rotation velocity measured using Doppler reflectometry in three ECH plasmas with constant densities: below, close to and above the threshold density, are shown in figure 1. At the threshold density a negative velocity well is measured at the radial position of maximum density gradient, which confirms the result obtained changing dynamically the plasma density. It is worth mentioning that the spontaneous inversion in the radial electric observed in low-density ECH plasmas is not a L–H transition (which involves, as discussed in section 4, higher values of radial electric field and E_r shear, a pronounced reduction in turbulence and an improvement in the energy confinement time). As reported in [14], the fluctuation levels and the turbulent transport increase as density increases up to the threshold value and slightly decrease as density further increases. The particle confinement time increases but no improvement in the energy confinement is observed [19].

In NBI plasmas, where the plasma density is higher ($\langle n_e \rangle$: (1.5–7) $\times$ 10^{19} m^{-3}), the radial electric field is negative in the whole plasma column and has substantial shear at the plasma edge. Profiles with a sheared radial electric field are observed in other helical systems before the L–H transition, which has been pointed out as a possible reason for the low power threshold of the H-mode in W7-AS [5, 6]. The radial profiles of the radial electric field for low and moderate density ECH plasmas, and high density NBI plasma measured by HIBP and Doppler reflectometry, are shown in figure 2. The perpendicular rotation velocity measured by Doppler reflectometry is a composition of both the plasma $E \times B$ velocity and the intrinsic phase velocity of the density fluctuations: $u_\perp = v_{E\times B} + v_{\rm ph}$. In cases in which the condition $v_{E\times B} \gg v_{\rm ph}$ holds, the radial electric field can be obtained directly from the perpendicular

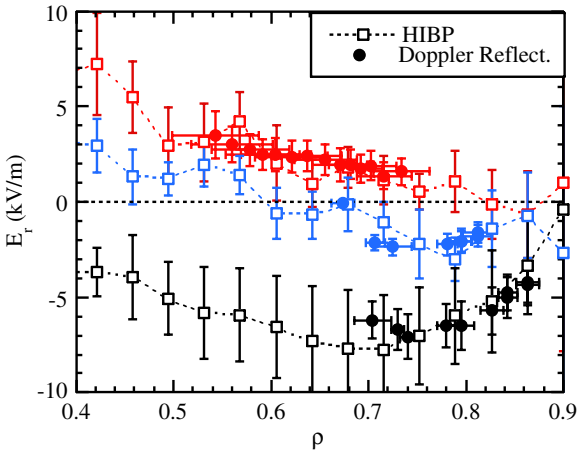

Figure 2. Radial profiles of the radial electric field measured by HIBP (empty symbols) and by Doppler reflectometry (filled symbols) for three plasma scenarios: ECH low density (top profiles (red) 300 kW, $\langle n_e \rangle = 0.43 \times 10^{19}$ m^{-3}), ECH moderate density (mid profiles (blue) 400 kW, $\langle n_e \rangle = 0.7 \times 10^{19}$ m^{-3}) and NBI high density (bottom profiles (black) 500 kW, $\langle n_e \rangle = 1.8 \times 10^{19}$ m^{-3}).

rotation velocity as $E_r = u_\perp B$. The good agreement found between the E_r profiles deduced from both diagnostics allows one to conclude that in the plasma region between $\rho = 0.5$ and $\rho = 0.9$, the Doppler reflectometry measurements are dominated by the $E \times B$ velocity,the intrinsic phase velocity of the density fluctuations being much smaller. Similar results have been found in the plasma edge of other devices [20, 21].

4. H-mode results

4.1. H-mode: transition conditions

H-mode transitions are achieved under NBI heating conditions when operating with lithium coated walls [8]. H-mode transitions reproduce common features found in other devices [5]: i.e. an increase in plasma density and plasma energy content, a reduction in H_α signal, the development of steep edge density gradients and a reduction in the turbulence level. They are observed at moderate input powers, with one (co-injector) and with two (co- and counter-) NBIs (about 500 kW port-through, each).

In order to estimate the 'quality' of the H-mode, a confinement enhancement factor H_{ISS04} is calculated as the ratio between the experimental global energy confinement time, τ_E, and the energy confinement time from the International Stellarator Scaling, τ_{ISS04} [22]. The dependence of the NBI absorbed power on the plasma density—as estimated using the FAFNER2 code that takes into account shine through, CX and ion losses—has been taken into account in the τ_E and τ_{ISS04} calculations. Confinement enhancement factors ranging from 0.9 to 1.3 are measured before the transition and increase to 1.1–1.5 during the H-mode, this relative increase being up to 30%.

To date, several different magnetic configurations have been explored, predominantly those with edge rotational transform values close to 1.6 ($n/m = 8/5$). As an example, figure 3 shows time traces of five discharges with different plasma densities, heated with the co-NBI, and for two different magnetic configurations (left panel $\iota(a) = 1.59$ and right panel $\iota(a) = 1.63$). From top to bottom the time evolution of the line-averaged density (a), the

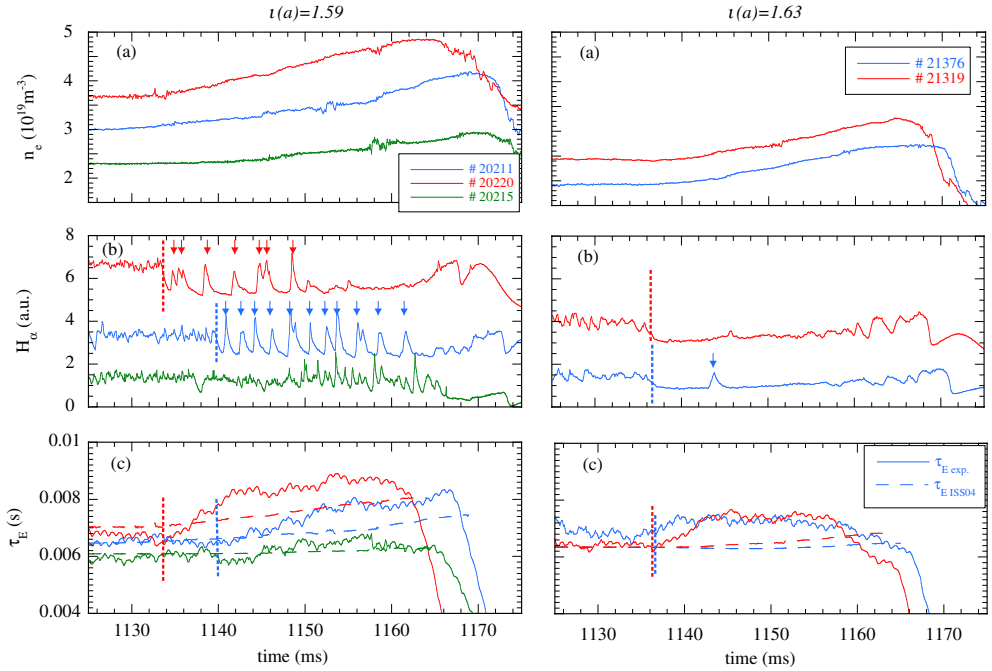

Figure 3. Time traces of five discharges with different plasma densities, heated with the co-NB injector, and for two different magnetic configurations (left panel $\iota(a) = 1.59$ and right panel $\iota(a) = 1.63$): (*a*) line-averaged density, (*b*) H_α signal and (*c*) experimental global energy confinement time, τ_E (solid lines) and energy confinement time from the International Stellarator Scaling τ_{ISS04} (dashed lines). Vertical dashed lines represent the L–H transition time and arrows point at ELMs. The H_α traces have been vertically displaced to facilitate a clearer representation.

H_α signal (b), τ_E and τ_{ISS04} (c) are shown. These examples reveal some differences between the transition characteristics in the two configurations. ELMy behaviour is frequently seen in the $\iota(a) = 1.59$ configuration that depends on the plasma density. At low densities ((2–2.5) $\times 10^{19}$ m^{-3}), the ELM repetition frequency is rather high, no clear drop in the H_α signal is seen and the confinement enhancement factor does not change significantly. In contrast, in the $\iota(a) = 1.63$ configuration, transitions are observed at low densities ((1.5–2.5) $\times 10^{19}$ m^{-3}) with few ELM events and with a higher increase in the H_{ISS04} factor. The relative increase in the confinement enhancement factor over the L-mode value is shown in figure 4 for several discharges heated with the co-NBI in these two magnetic configurations; the vacuum rotational transform profiles are also shown in figure 4. Although the dependence of the H-mode quality on edge rotational transform is not as pronounced as that found in W7-AS [5] or Heliotron J [23], in the $\iota(a) = 1.63$ magnetic configuration, enhancement factor increments of up to 30% are measured while maximum values of 20% are obtained in the $\iota(a) = 1.59$ magnetic configuration. It is worth noting that, although the rotational transform profile at the edge in the $\iota(a) = 1.59$ configuration is very close to the rational 8/5, the plasma current in these discharges is very low (about +0.3 kA) as is the corresponding increase in iota ($\Delta\iota(a) = 0.002$ using a cylindrical approximation).

Edge density profiles measured by AM reflectometry [24] with a time resolution of 2 ms, show an increase in the density gradient more pronounced in the $\iota(a) = 1.63$ configuration; at $\rho \approx 0.8$ the density gradient increases from about 2 to 6 $\times 10^{20}$ m^{-4} within 2–4 ms after

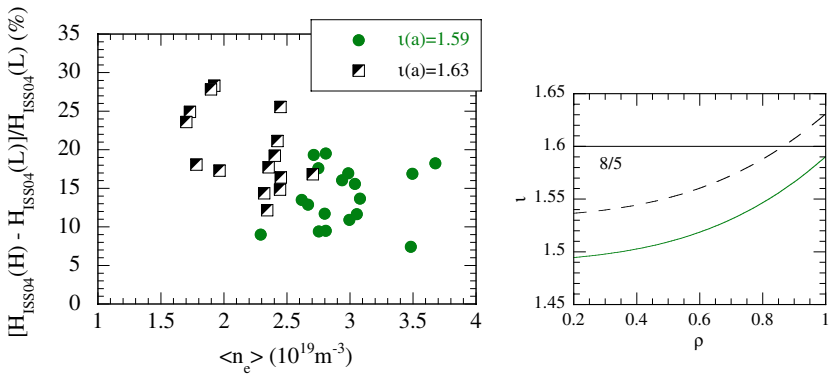

Figure 4. Left: relative increase in the confinement enhancement factor over the L-mode value for several discharges in $\iota(a) = 1.59$ (green dots) and in $\iota(a) = 1.63$ (black–white squares) magnetic configurations; right: vacuum rotational transform profiles in the two configurations.

the L–H transition, whereas it increases only up to $4 \times 10^{20}\,\mathrm{m}^{-4}$ (as measured 2–4 ms after the ELMy phase) in the $\iota(a) = 1.59$ configuration. Transport analysis has been done with the ASTRA system [25] using the experimental profiles of radiated power, plasma density, and electron and ion temperatures. Changes in the energy confinement time from about 7 to 8 ms are obtained, in agreement with those obtained experimentally. Particle confinement times close to 55 ms are obtained increasing by 25% and 35% in the magnetic configurations with $\iota(a) = 1.59$ and $\iota(a) = 1.63$, respectively.

4.2. E_r in H-mode NBI plasmas

At the L–H transition, an increase in the negative radial electric field and a significant reduction in the level of broadband density fluctuations are measured.

The perpendicular rotation velocity of the turbulence, as measured by Doppler reflectometry, is close to $-7\,\mathrm{km\,s}^{-1}$ in the electron diamagnetic direction at the radial range ρ: 0.7–0.85 and increases during the H-mode. The change in the perpendicular velocity is relatively modest in the $\iota(a) = 1.59$ configuration when compared with that in the $\iota(a) = 1.63$ configuration. Figure 5 shows the radial profiles of the perpendicular rotation velocity in L and H modes in both configurations. The L-mode profiles are measured 1–2 ms before the L–H transition while the H-mode ones are measured 6–8 ms after the L–H transition and after the ELMy phase, in the $\iota(a) = 1.63$ and $\iota(a) = 1.59$ configurations, respectively. Considering that the propagation velocity of the turbulence follows the $E \times B$ velocity, and taking into account that the magnetic field in this radial range is 0.9 T, an E_r field well of about $12\,\mathrm{kV\,m}^{-1}$ is measured at $\rho \approx 0.8$ in the $\iota(a) = 1.63$ configuration. At the transition, a factor of two reduction in the turbulence level is measured in these co-NBI heated plasmas.

The diamagnetic contribution to the radial electric field has been estimated using the experimental profiles. The diamagnetic term is close to the radial electric field obtained experimentally during the L-mode but it changes only very slightly after the transition. This result indicates that a $\boldsymbol{v} \times \boldsymbol{B}$ contribution appears in the H-mode and resembles that found in W7-AS [6].

In plasmas heated by both NBIs (with 900 kW port-through), an E_r field well of about $16\,\mathrm{kV\,m}^{-1}$ is measured at ρ: 0.8–0.85, about 3 cm inside the last closed flux surface. Although the E_r field well is weaker in TJ-II, its radial distance to $\rho = 1$ is comparable to those found in W7-AS and ASDEX-upgrade [5]. The position of the maximum shear in the perpendicular

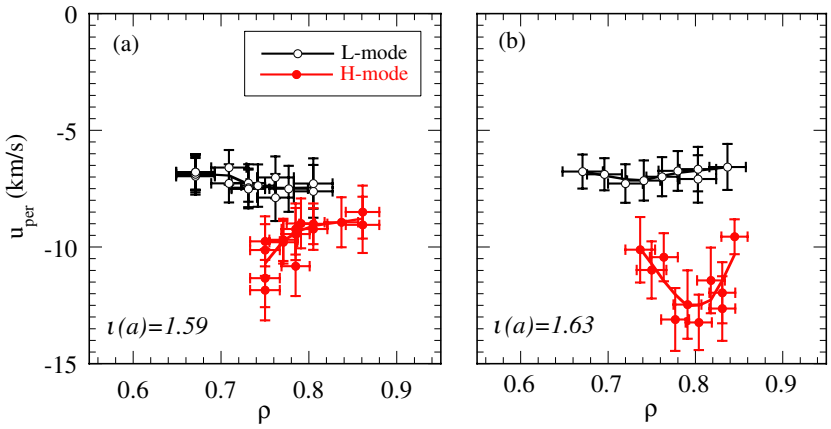

Figure 5. Radial profiles of the perpendicular rotation velocity in L and H modes in plasmas heated with co-NBI (400 kW port-through) in both configurations.

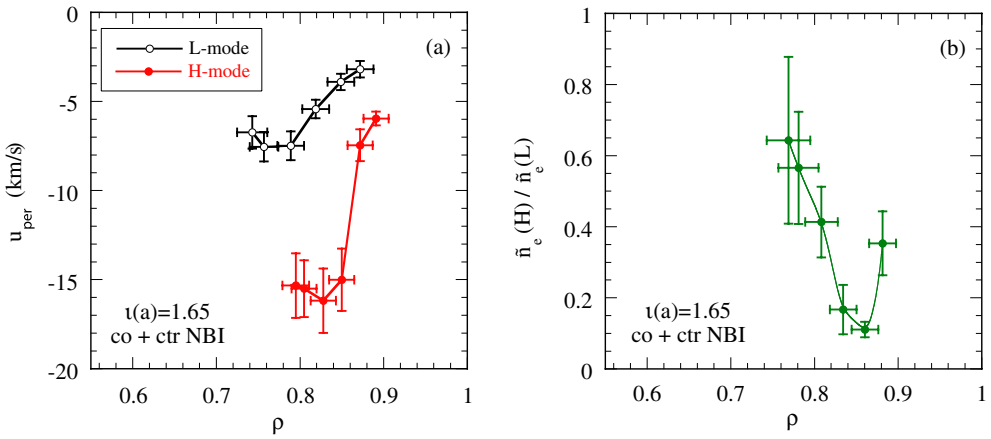

Figure 6. Radial profiles of the perpendicular rotation velocity in L and H modes (a) and density fluctuation reduction (b), in plasmas heated by both co- and counter-NBI (900 kW port-through) in the standard configuration $\iota(a) = 1.65$.

velocity is close to $\rho = 0.85$ and it is at this position where the maximum increase in the density gradient and the strongest reduction in the turbulence take place. Figure 6(a) shows the radial profiles of the perpendicular rotation velocity in L and H modes in a plasma heated with both co- and counter-NBI in the standard magnetic configuration with $\iota(a) = 1.65$. The fluctuation level, as given by the height of the Doppler peak, shows a factor of five reduction at the location of the maximum velocity shear. The ratio between the density fluctuations during the H and L modes is shown in figure 6(b).

4.3. Dynamics of radial electric field and turbulence

As has already been pointed out, Doppler reflectometry allows the study of the dynamics of the radial electric field, radial electric field shear and density fluctuations [11, 12]. In TJ-II, at the L–H transition, the radial electric field becomes more negative and a pronounced increase in the radial electric field shear is measured together with a reduction in plasma turbulence, as

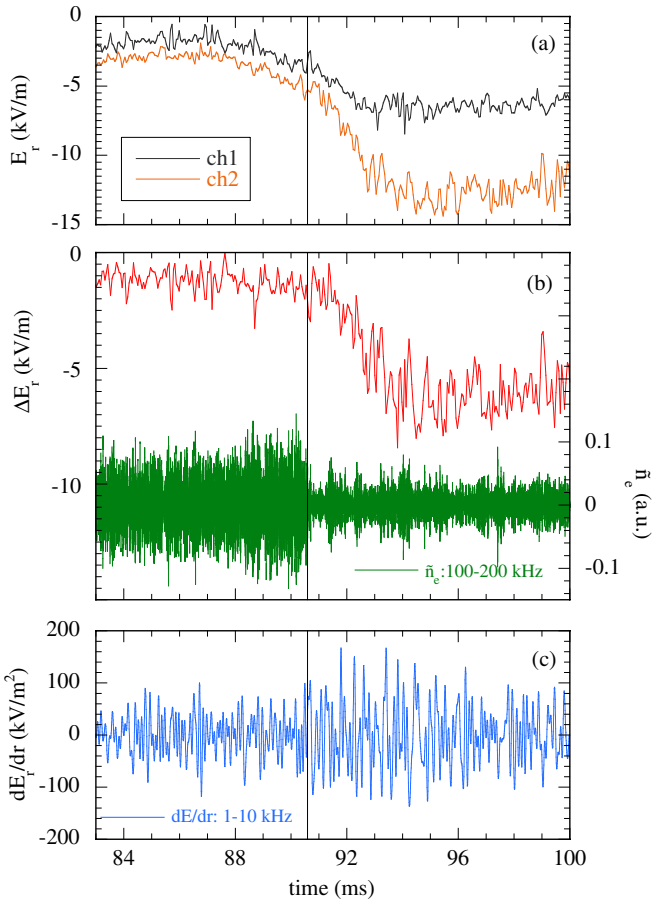

Figure 7. Time evolution of the radial electric field at two adjacent radial positions (*a*), their difference and the high frequency density fluctuations (*b*) and the low frequency fluctuations in the radial electric field shear (*c*); plasma heated by both NBIs (900 kW port-through) in the standard configuration $\iota(a) = 1.65$. The vertical line indicates the L–H transition time.

shown in figure 6. However, a closer look at the time evolution of both the radial electric field shear and the density fluctuations indicates that the reduction in density fluctuations precedes the increase in E_r field shear. This result resembles that recently found in JET [26] and seems to be in contradiction to numerous experimental observations supporting the paradigm of sheared electric field suppression of turbulence to explain transitions to improved confinement regimes [2, 27]. A detailed analysis of the signals reveals an increase in the fluctuations of the E_r field and E_r field shear within the frequency range 1–10 kHz just at the transition. The increase in the low frequency E_r fluctuations and the reduction in the high frequency density fluctuations are measured a few ms before the E_r field shear development. Figure 7(*a*) shows the time evolution of the E_r field at two adjacent radial positions; the difference between the E_r field at these two radial positions and the high frequency density fluctuations are shown in figure 7(*b*); finally, the evolution of the low frequency fluctuations in the E_r shear is shown in figure 7(*c*). The L–H transition time is indicated in the figure by a vertical line. This example indicates that the turbulence reduction precedes the increase in the mean sheared flow, but it is simultaneous with the increase in the low frequency oscillating sheared flow. This observation

may be an indicator, albeit insufficient, of the existence of zonal flows. As explained in [3, 4], additional three-dimensional measurements are required to assess the toroidal and poloidal symmetry of the oscillating sheared flows and their finite radial wavelength. In TJ-II, the degree of long-range similarity of density and potential fluctuations has been measured using the two Langmuir probes sets. Long-range correlations in the plasma potential reach values of up to 0.7–0.8 at the L–H transition whereas density fluctuations are always dominated by short-range scales [28]. These results are consistent with L–H transition models predicting plasma bifurcations triggered by zonal flows [29].

4.4. Influence of low order rational surfaces

The differences found when comparing the configurations discussed in section 4.1 suggest a possible role of the 8/5 rational surface on the transition. A $m = 5$ coherent mode is measured by the Mirnov coils during the L-mode in the $\iota(a) = 1.63$ configuration, which is stabilized right at the transition. In addition, pronounced oscillations in E_r are detected at the transition by the Doppler reflectometer that are absent in configurations without low order rational surfaces. These oscillations represent local changes in the E_r field which may be induced by the rational surface facilitating the transition and giving rise to steeper density gradients, a higher confinement enhancement factor and a deeper electric field well. In order to check the relation between the oscillations in E_r and the presence of a low order rational, additional experiments have been carried out in configurations with the 5/3 rational surface close to the plasma edge. Similar and even more pronounced E_r field oscillations have been detected at the transition. An example obtained in the $\iota(a) = 1.7$ magnetic configuration (5/3 close to $\rho = 0.8$) with the co-NB injector is shown in figure 8. The figure shows the time evolution of the radial electric field at two adjacent radial positions (figure 8(*a*)), the radial electric field shear (figure 8(*b*)) and the density fluctuation level (figure 8(*c*)). The L–H transition time is indicated in the figure by a vertical line. Fast and marked changes in the radial electric field are detected in the outer channel ($\rho \approx 0.8$ in figure 8(*a*)) giving rise to pronounced changes in the radial electric field shear (figure 8(*b*)); these changes start right at the transition where a reduction in the fluctuation level is detected (figure 8(*c*)). This result can be interpreted in terms of local changes in the radial electric field shear induced by the 5/3 rational surface which may facilitate or even trigger the transition. Further experiments are planned to investigate in more detail the role of the magnetic configuration in the L–H transition.

5. Conclusions

The behaviour of sheared flows has been experimentally studied in the TJ-II stellarator.

- In low-density ECH plasmas, Doppler reflectometry measurements indicate that the inversion in the radial electric field occurs at the radial position of maximum density gradient expanding towards the edge as the sheared flow is further developed.
- In higher density NBI L-mode plasmas the radial electric field is negative in the whole plasma column and a sheared radial electric field is observed at the plasma edge that is dominated by the diamagnetic component.
- L–H transitions are observed in NBI plasmas when operating under Li-coated walls:
  - L–H transitions observed in magnetic configurations with and without the 8/5 rational surface close to the plasma edge show differences in density gradients, sheared flows and confinement enhancement factor. The observations may be interpreted in terms of local changes in the radial electric field induced by the rational surface that could

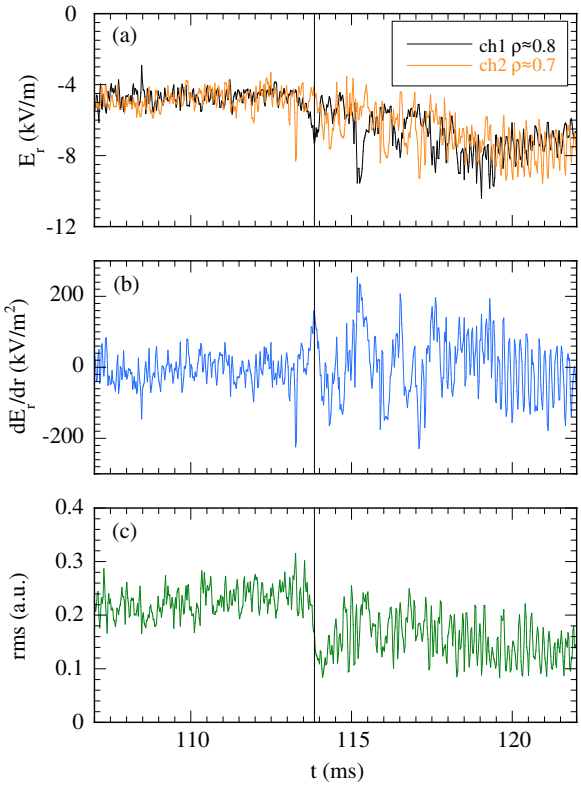

Figure 8. Time evolution of the radial electric field at two adjacent radial positions (*a*), E_r field shear (*b*) and density fluctuations (*c*), in a magnetic configuration with the rational surface 5/3 close to $\rho = 0.8$ and with co-NBI (400 kW port-through). The vertical line indicates the L–H transition time.

facilitate the L–H transition. Similar behaviour has been observed in configurations with the 5/3 rational surface close to the plasma edge.

– Fluctuation measurements show a reduction in the turbulence level that is most pronounced at the position of maximum E_r shear. High temporal and spatial resolution measurements indicate that turbulence reduction precedes the increase in the mean shear flow, but is simultaneous with the increase in the low frequency oscillating shear flow. These observations are consistent with L–H transition models predicting plasma bifurcations triggered by zonal flows.

Acknowledgments

The authors acknowledge the entire TJ-II team for their support during the experiments. This work has been partially funded by the Spanish Ministry of Science and Innovation under contract number ENE2007-65727.

References

[1] Biglari H, Diamond P H and Terry P W 1990 *Phys. Fluids* B **2** 1
[2] Groebner R J, Burrel K H and Seraydarian R P 1990 *Phys. Rev. Lett.* **64** 3015–8

[3] Diamond P H, Itoh S-I, Itoh K and Hahm T S 2005 *Plasma Phys. Control. Fusion* **47** R35–R161
[4] Fujisawa A 2009 *Nucl. Fusion* **49** 013001
[5] Wagner F 2007 *Plasma Phys. Control. Fusion* **49** B1–B33
[6] Wagner F, Hirsch M, Hartfuss H J, Laqua H P and Maassberg H 2006 *Plasma Phys. Control. Fusion* **48** A217–39
[7] Sánchez J *et al* 2009 *Nucl. Fusion* **49** at press
[8] Tabarés F *et al* 2008 *Plasma Phys. Control. Fusion* **50** 124051
[9] Fernández A, Kasparek W and Likin K 2001 *Int. J. Infrared Millim. Waves* **22** 649
[10] Happel T *et al* 2009 *Rev. Sci. Instrum.* **80** 073502
[11] Hirsch M *et al* 2006 *Plasma Phys. Control. Fusion* **48** S155
[12] Schirmer J, Conway G D, Zhom H and Suttrop W 2006 *Nucl. Fusion* **46** S780
[13] Krupnik L *et al* 2003 *Proc 30th European Conf. on Controlled Fusion and Plasma Physics (St Petersburg, Russia, July 2003)* (on CD-ROM)
[14] Pedrosa M A *et al* 2008 *Phys. Rev. Lett.* **100** 215003
[15] Hidalgo C, Pedrosa M A, García L and Ware A 2004 *Phys. Rev.* E **70** 067402
[16] Estrada T, Blanco E, Cupido L, Manso M E and Sánchez J 2006 *Nucl. Fusion* **46** S792
[17] Melnikov A V *et al* 2007 *Fusion Sci. Technol.* **51** 31
[18] Happel T, Estrada T and Hidalgo C 2008 *Europhys. Lett.* **84** 65001
[19] Vargas V I *et al* 2009 Density dependence of particle transport in ECH plasmas of the TJ-II stellarator *Informes Técnicos Ciemat* No 1162
[20] Hirsch M *et al* 2001 *Plasma Phys. Control. Fusion* **43** 1641
[21] Conway G D *et al* 2004 *Plasma Phys. Control. Fusion* **46** 951
[22] Yamada H *et al* 2005 *Nucl. Fusion* **45** 1684
[23] Sano F *et al* 2005 *Nucl. Fusion* **45** 1557
[24] Estrada T *et al* 2001 *Plasma Phys. Control. Fusion* **43** 1535
[25] Pereverzev G V and Yushmanov P N 2002 ASTRA Automated system for transport analysis *Report* IPP 5/98, Max-Planck-Institut für Plasmaphysik, Garching
[26] Andrew Y *et al* 2008 *Europhys. Lett.* **83** 15003
[27] Burrel K H 1997 *Phys. Plasmas* **4** 1499
[28] Hidalgo C *et al* 2009 *Europhys. Lett.* submitted
[29] Kim E and Diamond P H 2003 *Phys. Plasmas* **10** 1698